Bartłomiej Ćmielewski*, Izabela Wilczyńska,
Ciechosław Patrzałek***, Jacek Kościuk******

Digital close-range photogrammetry of El Fuerte de Samaipata

Cyfrowa fotogrametria bliskiego zasięgu El Fuerte de Samaipata

Introduction

El Fuerte de Samaipata is an archaeological site in the department of Santa Cruz in Bolivia, located on a rocky hill at an altitude of about 1950 m above sea level. The site was constructed and occupied by the Mojocoyas culture in the fourth century, and it was during this time that the rock began to be carved. In the 15th century, the site was conquered by the Inca, who made it a provincial capital. The strategic location of the site was also recognised by the Spaniards, who made it an important staging post on the road from Asunción and Santa Cruz to La Plata (modern Sucre), Cochabamba, and Potosí (where silver mines were located) [1].

The archaeological site consists of two parts: the ceremonial part (14th–16th centuries), and the area to the south – the residential and administrative part. The ceremonial part is a sculpted rock that is 250 m long and 60 m wide, which makes it one of the largest collection of petroglyphs in the world. The sandstone was carved to create niches, canals, and zoomorphic designs such as snakes and wild cats like pumas and jaguars [2].

In this article, we present the results of using a non-metric camera as a tool in terrestrial close-range photogrammetry for documentation of El Fuerte de Samaipata as part of the project "Architectural examination and complex documentation of Samaipata (Fuerte de Samaipata/Bolivia). The place on the World Heritage List", funded by The National Science Centre Poland.

Methods

Nowadays, 3D data are extremely useful for permanently storing and documenting important sites in digital form. Sometimes, they may be the last form to be passed to the next generations (for example, as heritage may be destroyed in wars). With technical progress, a large number of projects now have complete digital models [3]–[8]. Remote sensing technologies and methodologies are common for cultural heritage 3D documentation and modeling [9]. They allow very realistic 3D models (in terms of geometric and radiometric accuracy) to be generated. Such models can be used for many purposes, including historical documentation [10], [11], preservation and conservation [12], [13], cross-comparisons, monitoring shape and colour, virtual reality applications [14], [15], 3D repositories, web-based Geographic Information System (GIS), computer-aided restoration [16], multimedia exhibitions [17], and simple visualisations.

The documentation and conservation of cultural heritage depends on the availability of means and resources. Data repositories allow the present state of a site to be described and provide metrical information, which is useful for direct restoration of objects. Nowadays, digital photogrammetry is used in many applications, especially in

---

* ORCID: 0000-0002-1035-3905. Faculty of Architecture, Wrocław University of Science and Technology, e-mail: bartlomiej.cmielewski@pwr.edu.pl

** ORCID: 0000-0002-1397-8118. Faculty of Environmental Engineering and Geodesy, Wrocław University of Environmental and Life Sciences.

*** ORCID: 0000-0002-0853-5494. Faculty of Environmental Engineering and Geodesy, Wrocław University of Environmental and Life Sciences.

**** ORCID: 0000-0003-0623-8071. Faculty of Architecture, Wrocław University of Science and Technology.
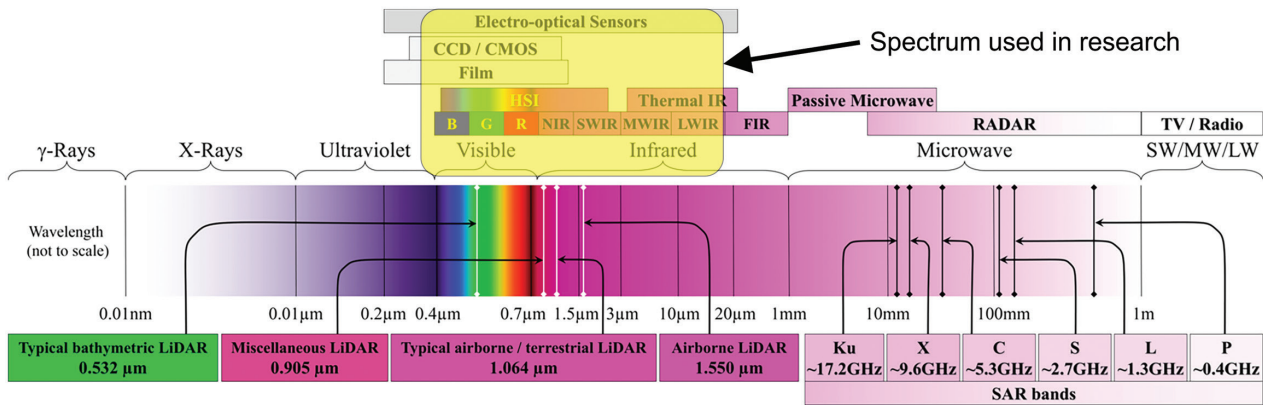
Fig. 1. Electromagnetic (EM) spectrum (after: [25])

cartography and mapping. It is also used for precise 3D documentation of cultural heritage [5], [11], [18]–[20], reverse engineering, monitoring and deformation analyses of structures [21], human movement analyses [22], industrial measurements [23], urban planning, and forensic analyses [24]. Innovations in the field of photogrammetry, especially matching algorithms, increase of the quality of spatial data obtained by images.

Sensors

Remote sensing involves the sensing of energy in parts of the electromagnetic spectrum (Fig. 1), which is the continuous range of electromagnetic radiation from gamma rays, through visible light, to radio waves.

To create documentation for archaeological, architectural, and conservation purposes, it is common to use multispectral or hyperspectral sensors that provide images from satellites. These are commonly considered in literature to be successful [26]. Other solutions are based on terrestrial cameras, which also provide good results [27]–[29].

While RGB orthoimages are used for documentation purposes, another indicator, the Normalised Difference Vegetation Index (NDVI), is commonly used in remote sensing measurements and allows the developmental state and condition of vegetation to be determined. Vegetation interacts with solar radiation, weather conditions, and the nutrients and water content on its roots (usually from soil). The NDVI can show where soil has more moisture (which can indicate underground constructions like hidden walls) or places that have been degraded by vegetation – like in the case of Samaipata. The NDVI is based on the contrast between the largest reflection in the near-infrared band (which vegetation strongly reflects) and the red band (which vegetation absorbs). The indicator was used for the first time by John W. Rouse *et al.* in 1973 [30] and is calculated according to the following formula (1):

$$NDVI = \frac{(NIR - VIS)}{(NIR + VIS)} \tag{1}$$

where:
    VIS – reflection in the red band,
    NIR – reflection in the near-infrared band.

Vibrant, green plants absorb photosynthetically active solar radiation in the range of 0.4–0.7 μm. Radiation with longer wavelengths (0.7–1.1 μm) is absorbed to a small extent. The NDVI ranges from –1 to 1. Higher index values correspond to a higher reflection in the near-infrared range and a smaller reflection in the red range. A high value of the indicator corresponds to areas covered with lush vegetation in good condition [31].

Materials and methods

RGB camera

For the close-range photogrammetry, we used an ILCE-7RM2 DSLR camera from Sony. It has a full frame (35.9 × 24.0 mm) CMOS Exmor R® sensor and effective resolution of 42.4 megapixels (image resolution 7952 × 5304). The pixel dimension is 4.53 × 4.53 μm, which provides good sensitivity.

Multispectral camera

For multispectral analysis, we used a Parrot Sequoia camera equipped with four monochrome sensors and one RGB sensor. The monochrome sensors (global shutter, 1.2 megapixels) collect data in discrete spectral bands: green (550 nm with 40 nm bandwidth), red (660 nm with 40 nm bandwidth), red edge (735 nm with 10 nm bandwidth) and near infrared (790 nm with 40 nm bandwidth). The RGB sensor (rolling shutter) has a 16 megapixel resolution (4608 × 3456) with a focal length of 4.88 mm. It is complemented by a sunshine sensor with four spectral sensors (the same filters as the body), and GPS, IMU, and magnetometer sensors for direct geotagging.

Thermal camera

For thermal analysis, a Flir Tau 2 324 VOx Microbolometer, f/13 mm, 9 Hz camera was used. It has a pixel size of 25 μm with a better performance than 50 mK at f/1.0. The sensing spectral band is from 7.5 to 13.5 μm and advanced radiometry was also enabled. The TeAx Thermalcapture module was attached to the camera for direct
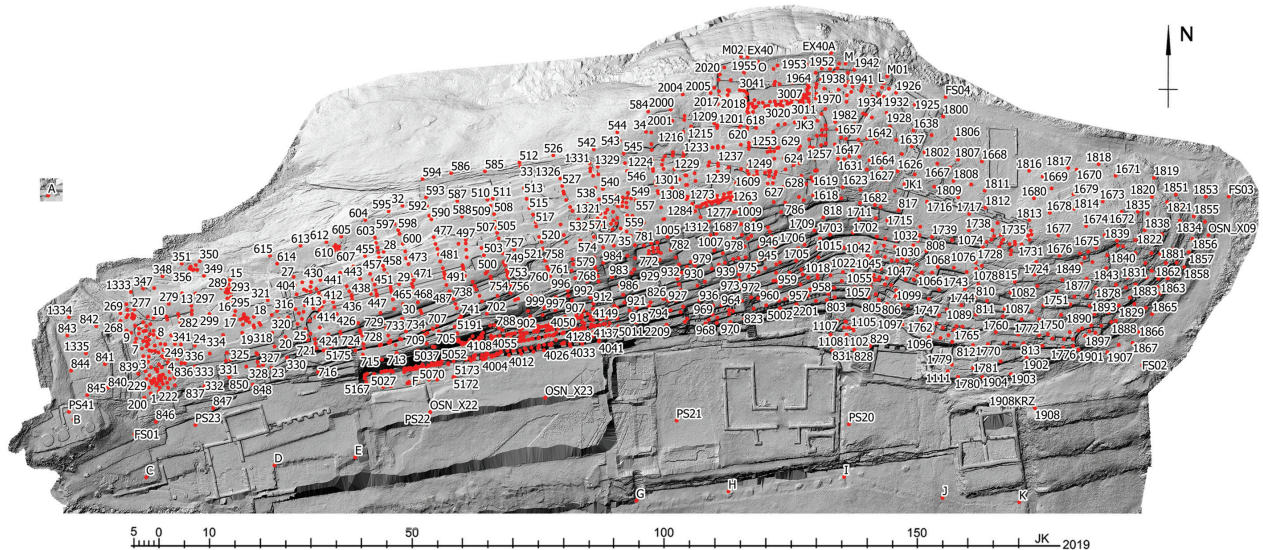
Fig. 2. Survey point distribution (elaborated by B. Ćmielewski)

geotagging (from GPS times and coordinates) of images that were loaded onto an external USB memory.

Survey network

The first step was to perform a survey, so we used a Leica TCRP1203 total station with an angular accuracy of 3 arcsec and a distance error of 5 mm + 2 mm. Next, we processed the data in local coordinates, and later these were adjusted to the network. The final step was to transform the coordinates from the local to the global reference frame using isometric transformation to the WGS 84/UTM zone 20S, EPSG:32720 coordinate system and GPS points FS01, FS02, FS03, and FS04. After adjustment, the worst point average square position error was 6.8 mm and the worst point average square height error was 2.9 mm. Using these adjusted and transformed coordinates, the photogrammetric network was measured and adjusted. The total number of photogrammetric points was over 1500, and their distribution on the site is presented in Figure 2.

Photogrammetry processing results and workflow

All acquired data was processed in one of the best pieces of software on the market – Agisoft Photoscan Professional. The workflow is presented in Figure 3.

The first step after importing images was to calculate the image quality and remove the lowest quality images. Next, photos were aligned. For high RGB resolutions, the key point limit was set to 40,000 and the tie point limit was set to 3,000. For multispectral low-resolution images, the key point limit was set to 80,000 and the tie point limit was set to 10,000. Such settings allowed sustainable image quality and cloud computing power to be used. After alignment, the markers were loaded, and the tedious process of pointing markers in pictures started. Next, optimisation was applied to recalculate the lens equitation and camera location. After this step, the error value was checked and the gradual calculation of the reconstruction uncertainty value of tie points was calculated. After removing values over 100, optimisation was conducted again. This step was repeated a few times
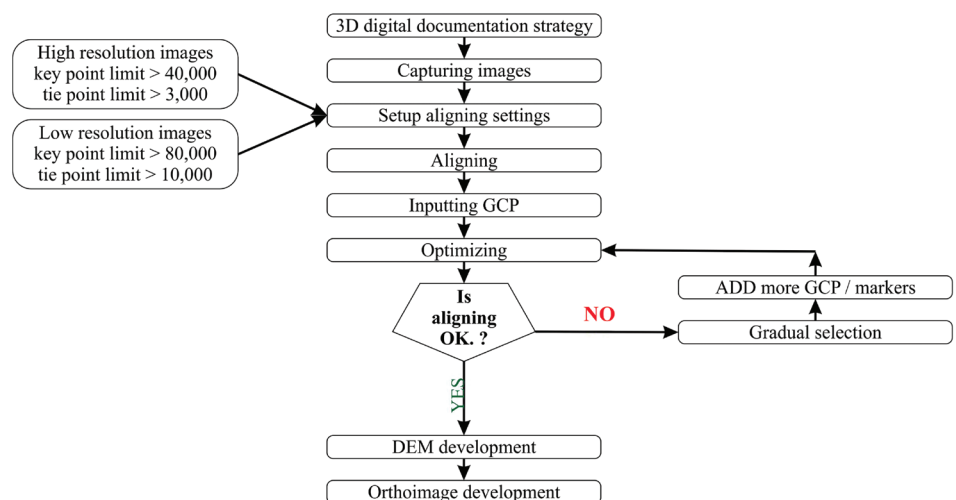

Fig. 3. Workflow for image processing (elaborated by B. Ćmielewski)

Table 1. Summary of photogrammetric projects (elaborated by B. Ćmielewski)

Photo-alignment	RGB	Multispectral
Camera stations	51,128	110,684 (4 × 27,671)
Camera altitude	2.36 m	3.34 m
Coverage area	0.0292 km²	0.0213 km²
Ground resolution	0.292 mm/pixel	3.16 mm/pixel
Tie points	23,071,218	51,607,684
Projections	118,482,378	634,582,165
Reprojection error	0.647 pixels	1.14 pixels
Max reprojection error	125.92 pixels (36,77 mm)	78.69 pixels (248,66 mm)
Key points	161.48 GB	259.761 GB
Matching time	22 days 7 hours	25 days 14 hours
Alignment time	3 days 11 hours	1 hours 46 minutes
Optimisation time	37 minutes 53 seconds	5 hours 11 minutes
DEM	RGB	Multispectral
Size	14,267 × 5,642 pixel	19,744 × 7,359 pixel
Processing time	10 minutes 20 seconds	30 minutes 57 seconds
Resolution	1.91 cm/pixel	1.22 cm/pixel
Point density	0.274 points/cm²	0.673 points/cm²
Orthoimage	RGB	Multispectral
Size	931,971 × 368,254 pixel	76,075 × 28,216 pixel
Processing time	5 days 21 hours	1 days 0 hours
Colours	3 bands, uint8	4 bands, uint16
Raster Transform Expression	–	((B4-B2)/(B4+B2))+0.25

with the additional action of adding common points in places where the tie point cloud and image location were "strange" – meaning that the reconstructed location of images could not have been in such a position, or the point cloud was divided, which happened in particular when the multispectral low-resolution images were processed.

After achieving satisfying results – flat point cloud and low error value on check and control points – we created a digital elevation model (DEM) and later an orthoimage of the rock. The main statistics of processing both RGB and multispectral images are presented in Table 1.

There were over 1500 applied markers. Some of them were used as controls and some as check points, and the selection of both types of points were specially selected to evenly cover the rock area. The error values are summarised in Table 2. The average 3D error both control and check points for the RGB project was around 1.5 cm, and for the multispectral project, 3 cm. The photogrammetric project allowed the archaeological site to be reconstructed with an accuracy of centimetres and a very high resolution of the final orthoimage at the level of 0.3 mm. This resolution, as presented in Figure 4, allowed individual blades of grass to be counted.

Using multispectral cameras with NDVIs, we can highlight the places where vegetation is accelerating the erosion process (Fig. 5).

Thermal documentation

We had problems with thermally documenting the whole archaeological site, as it was not possible to capture the entire site at one time. The thermal colours on the images depend on temperature, which depends on environmental conditions. We were not able to fly a drone over the whole site due to very strong wind. We could only produce an orthoimage for part of the site captured in a relatively short period of time. The example given in Figure 6 presents part of a vertical wall facing south from sector S08[1].

Conclusions

The results of these remote sensing studies are not only important documentation showing the current state of El Fuerte de Samaipata, but also form the basis for further studies. The detailed survey network established for this project was also used during the 3D laser scanning of the Samaipata rock.

---

[1] Cf. J. Kościuk, G. Orefici, M. Ziółkowski, A. Kubicka, R. Muñóz Risolazo, *Description and analysis of El Fuerte de Samaipata in the light of new research, and a proposal of the relative chronology of its main elements*, in the same issue of "Architectus".
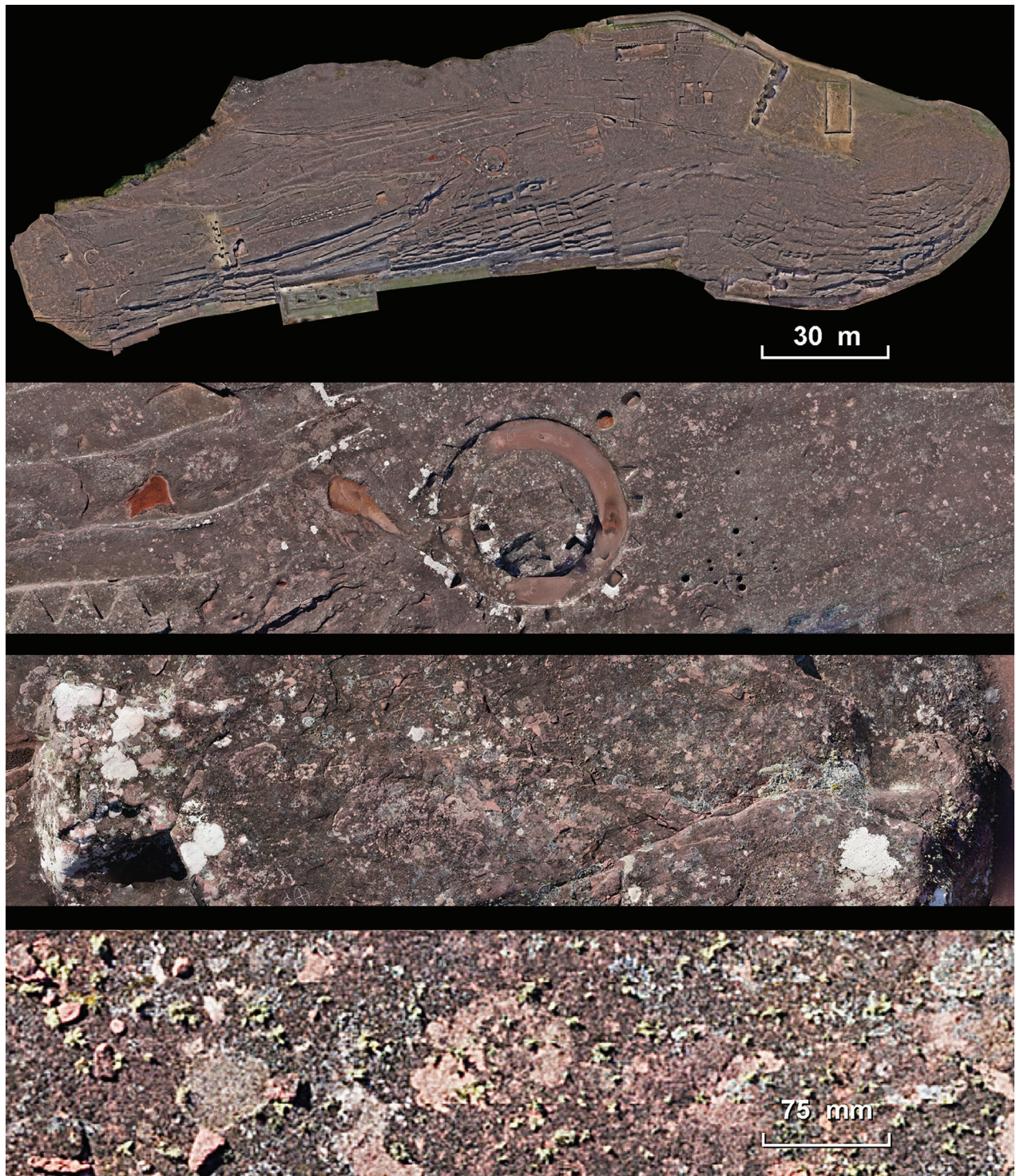
Fig. 4. View of the Samaipata rock followed by images zoomed into the central part of the main orthoimage (elaborated by B. Ćmielewski)

The high-resolution orthoimage was, together with the results of 3D laser scanning, the basis for drawing up a detailed CAD plan of all the terraces, niches, reservoirs, canals, and petroglyphs densely covering the entire rock surface. As both the photogrammetric studies and 3D laser scanning results were embedded in an analogous coordinate system that guaranteed their correlation, they were extremely important when preparing the vector plan. Some details of the complex were better visible either on the orthoimages made on the basis of photogrammetric studies or on orthoimages obtained from terrestrial laser scanning (TLS). In a few cases, the best source for interpreting the most eroded features were digital terrain model (DTM) images rendered with hill-shading algorithms.

Multispectral orthoimages also proved to be extremely useful – they allowed the current state of the spreading of lichen, fungi, and algae attacking the surface of the rock to be documented. In the future, if such a study is repeated, the orthoimages produced in this project will allow the speed of progressing biological erosion to be determined.

Table 2. Accuracy of control and check points in photogrammetric projects (elaborated by B. Ćmielewski)

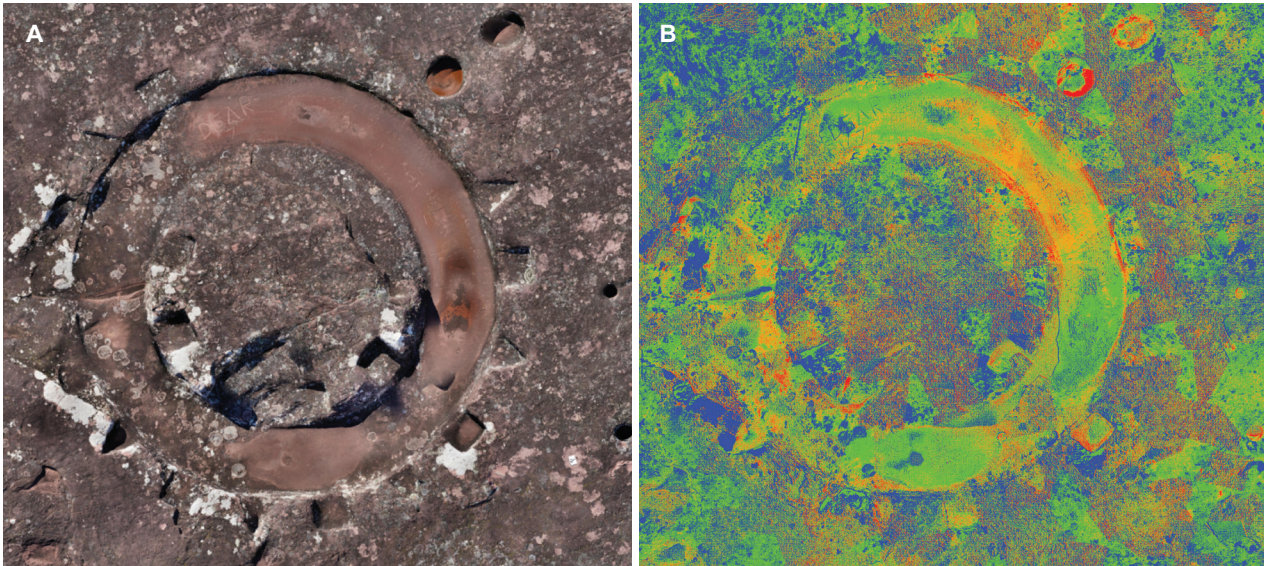|	RGB project accuracy					Multispectral project accuracy				
	x error [cm]	y error [cm]	z error [cm]	xy error [cm]	total [cm]	x error [cm]	y error [cm]	z error [cm]	xy error [cm]	total [cm]
Control points RMSE	0.934	1.076	2.628	1.426	2.989	2.447	1.705	2.527	2.983	3.910
Check points RMSE	0.855	1.112	3.560	1.403	3.827	2.654	1.956	3.532	3.297	4.832

Fig. 5. Comparison of RGB (A) and multispectral (B) orthoimages
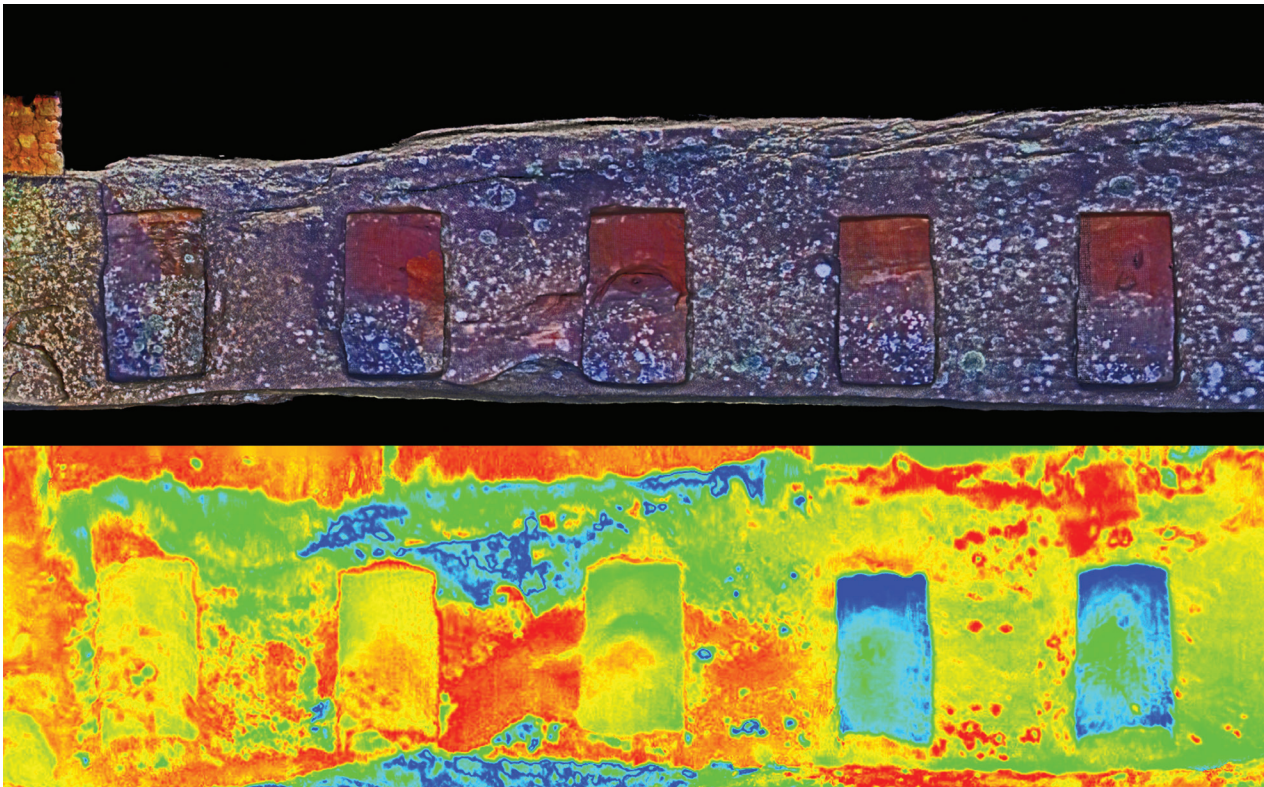(elaborated by B. Ćmielewski)

Fig. 6. Juxtaposition of the RGB and thermal images
(elaborated by J. Kościuk)

If a restoration project ever starts, the results obtained by us will be an important reference material to monitor the effectiveness of actions taken.

An important limitation and drawback of the research was the choice of season in which the measurements were taken. Theoretically, June and July should be the months of the lowest precipitation in Samaipata. However, the 2016 season was unusual in this respect – during our 60-day stay, we recorded only 20 days without rainfall. In addition, unusually strong winds did not allow us to use the drone, which in turn forced the team to take almost 40,000 photos from ground level. This number of photos obviously had to result in longer photogrammetric calculations.

Periodic monitoring of the state of preservation of El Fuerte using the methods presented here seems worth recommending. However, the choice of future dates for this monitoring should be guided by the forecast for wind and not for precipitation. In favourable weather conditions, a drone could collect all the material necessary for a photogrammetric project of this size within no more than one day of flights.

References / Bibliografia

[1] *El Fuerte de Samaipata*, https://whc.unesco.org/en/list/883/ [accessed: 26.08.2019].

[2] *Skarby świata: 890 pomników kultury i przyrody z Listy Światowego Dziedzictwa UNESCO*, J. Egert-Romanowska, K. Duran, M. Kalinowska (wyd.), Wydawnictwo Naukowe PWN, Warszawa [2010].

[3] Levoy M., Pulli K., Curless B. *et al.*, *The Digital Michelangelo Project: 3D Scanning of Large Statues*, [in:] J.R. Brown, K. Akeley (chairmans), *Proceedings of SIGGRAPH'00, The 27th International Conference on Computer Graphics and Interactive Techniques" 23–28 July 2000, New Orleans, LA, USA*, ACM Press–Addison-Wesley Publishing, New York, NY, 2000, 131–144, doi: 10.1145/344779.344849.

[4] Bernardini F., Rushmeier H., Martin I.M., Mittleman J., Taubin G., *Building a digital model of Michelangelo's Florentine Pieta*, "IEEE Computer Graphics and Applications" 2002, Vol. 22, Iss. 1, 59–67, doi: 10.1109/38.974519.

[5] Gruen A., Remondino F., Zhang L., *Photogrammetric reconstruction of the Great Buddha of Bamiyan, Afghanistan*, "The Photogrammetric Record" 2004, Vol. 19, Iss. 107, 177–199, doi: 10.1111/j.0031-868X.2004.00278.x.

[6] Guidi G., Beraldin J.A., Atzeni C., *High accuracy 3D modelling of cultural heritage: The Digitizing of Donatello's "Maddalena"*, "IEEE Transactions on Image Processing" 2004, 13, 370–380, doi: 10.1109/tip.2003.822592.

[7] El-Hakim S., Beraldin J., Remondino F., Picard M., Cournoyer L., Baltsavias E., *Using Terrestrial Laser Scanning and Digital Images for the 3D Modelling of the Erechteion, Acropolis of Athens*, [in:] *Proceedings of DMACH Conference on Digital Media and its Applications in Cultural Heritage, 3–6 November 2008, Amman, Jordan*, Amman 2008, 3–16, https://www.semanticscholar.org/paper/Using-Terrestrial-Laser-Scanning-and-Digital-Images-El-Hakim-Beraldin/06d006e5ebbe109db04cca877cd0991c6c440dd6.

[8] Remondino F., El-Hakim S., Girardi S., Rizzi A., Benedetti S., Gonzo L., *3D Virtual Reconstruction and Visualization of Complex Architectures – The 3D-ARCH Project*, "The International Archives of the Photogrammetry, Remote Sensing and Spatial Information Sciences" 2009, Vol. XXXVIII-5/W1, https://www.isprs.org/proceedings/XXXVIII/5-W1/pdf/remondino_etal.pdf.

[9] *Remote Sensing for Archaeological Heritage Management. Proceedings of the 11th EAC Heritage Management Symposium, Reykjavík, Iceland, 25–27 March 2010*, D.C. Cowley (ed.), Europae Archaeologia Consilium, Association Internationale sans But Lucratif, Siège social, Bruxelles 2011.

[10] Doneus M., Neubauer W., *Laser scanners for 3D documentation of stratigraphic excavations*, [in:] M. Baltsavias, A. Gruen, M. Pateraki, L. Van Gool (eds.), *Recording, Modeling and Visualization of Cultural Heritage. Proceedings of the International Workshop, Centro Stefano Franscini, Monte Verita, Ascona, Switzerland, May 22–27, 2005*, Taylor & Francis, London 2006, 193–204.

[11] El-Hakim S., Gonzo L., Voltolini F. *et al.*, *Detailed 3D modelling of castles*, "International Journal of Architectural Computing" 2007, Vol. 5, Iss. 2, 199–220, doi: 10.1260/1478-0771.5.2.200.

[12] Akca D., Remondino F., Novak D., Hanusch T., Schrotter G., Gruen A., *Recording and Modelling of Cultural Heritage Objects with Coded Structured Light Projection Systems*, [in:] S. Campana (ed.), *From space to place. 2. International Conference on Remote Sensing in Archaeology. Proceedings of the 2. international workshop, CNR, Rome, Italy, December 2–4, 2006*, Archaeopress, Oxford 2006, 375–382.

[13] Remondino F., Rizzi A., Agugiaro G. *et al.*, *Geomatics and Geoinformatics for Digital 3D Documentation, Fruition and Valorization of Cultural Heritage*, [in:] *Proceedings of EUROMED 2010 Workshop "Museum Futures: Emerging Technological and Social Paradigms", 8–13 November 2010, Lemessos, Cyprus*, https://www.researchgate.net/publication/323245824_Geomatics_and_Geoinformatics_for_the_Digital_3D_Documentation_Fruition_and_Valorization_of_Cultural_Heritage [accessed: 14.06.2019].

[14] *Virtual Reality in Archaeology*, A. Barceló, M. Forte, D.H. Sanders (eds.), BAR International Series, Oxford 2000.

[15] Bruno F., Bruno S., De Sensi G., Luchi M.L., Mancuso S., Muzzupappa M., *From 3D reconstruction to virtual reality: A complete methodology for digital archaeological exhibition*, "Journal of Cultural Heritage" 2010, Vol. 11, Iss. 1, 42–49, doi: 10.1016/j.culher.2009.02.006.

[16] Fowles P.S., Larson J.H., Dean C., Solajic M., *The laser recording and virtual restoration of a wooden sculpture of Buddha*, "Journal of Cultural Heritage" 2003, Vol. 4, Suppl. 1, 367–371, doi: 10.1016/S1296-2074(02)01141-X.

[17] Remondino F., Rizzi A., Girardi S., Petti F., Avanzini M., *3D ichnology – Recovering digital 3D models of dinosaur footprints*, "The Photogrammetric Record" 2010, Vol. 25, Iss. 131, 266–282, doi: 10.1111/j.1477-9730.2010.00587.x.

[18] Yastikli N., *Documentation of cultural heritage using digital photogrammetry and laser scanning*, "Journal of Cultural Heritage" 2007, Vol. 8, Iss. 4, 423–427, doi: 10.1016/j.culher.2007.06.003.

[19] Themistocleous K., Ioannides M., Agapiou A., Hadjimitsis D.G., *The methodology of documenting cultural heritage sites using photogrammetry, UAV, and 3D printing techniques: the case study of Asinou Church in Cyprus*, [in:] D.G. Hadjimitsis, K. Themistocleous, S. Michaelides, G. Papadavid (eds.), *Proceedings of Spie. Third International Conference on Remote Sensing and Geoinformation of the Environment (RSCy2015). 16–19 March 2015, Paphos, Cyprus*, Vol. 9535, Spie, [Washington 2015], doi: 10.1117/12.2195626.

[20] Dhonju H.K., Xiao W., Sarhosis V. *et al.*, *Feasibility Study of Low-Cost Image-Based Heritage Documentation in Nepal*, "The International Archives of the Photogrammetry, Remote Sensing and Spatial Information Sciences" 2017, Vol. XLII-2/W3, 237–242, doi: 10.5194/isprs-archives-XLII-2-W3-237-2017.

[21] Hampel U., Maas H.G., *Application of Digital Photogrammetry for Measuring Deformation and Cracks during Load Tests in Civil Engineering Material Testing*, [in:] A. Gruen, H. Kahmen (eds.), *Optical 3-D measurement techniques. Applications in GIS, mapping, manifactoring, quality control, robotics, navigation, mobile*

mapping, medical imaging, VR generation and animation. Papers presented on 6th Conference on Optical 3D Measurement Techniques", Zurich, Switzerland, 22–25 September 2003, Chair of Photogrammetry and Remote Sensing, Institute of Geodesy and Photogrammetry, ETZ, Zürich 2003, Vol. 2, 80–88, https://www.semanticscholar.org/paper/APPLICATION-OF-DIGITAL-PHOTOGRAMMETRY-FOR-MEASURING-Hampel-Maas/c585e-7041596be195c6c9b350aef4139f53769dc.

[22] D'Apuzzo N., *Surface Measurement and Tracking of Human Body Parts from Multi Station Video Sequences*, Ph.D. Thesis, Institute of Geodesy and Photogrammetry, ETH, Zürich 2003.

[23] Luhmann Th., *Close range photogrammetry for industrial applications*, "ISPRS Journal of Photogrammetry and Remote Sensing" 2010, Vol. 65, Iss. 6, 558–569, doi: 10.1016/j.isprsjprs.2010.06.003.

[24] Gonzalez-Aguilera D., Gomez-Lahoz J., *Forensic terrestrial photogrammetry from a single image*, "Journal of Forensic Sciences" 2009, Vol. 54, Iss. 6, 1376–1387, doi: 10.1111/j.1556-4029.2009.01170.x.

[25] Toth C., Jóźków G., *Remote sensing platforms and sensors: A survey*, "ISPRS Journal of Photogrammetry and Remote Sensing" 2016, Vol. 115, 22–36, doi: 10.1016/j.isprsjprs.2015.10.004.

[26] Lasaponara R., Masini N., *Satellite Remote Sensing in Archaeology: past, present and future*, "Journal of Archaeological Science" 2011, Vol. 38, Iss. 9, 1995–2002, doi: 10.1016/j.jas.2011.02.002.

[27] Batic J. *et al.* (eds.), *Photogrammetry as a Method of Documenting the Cultural Heritage*, Ministry of Culture, Ljubljana 1996.

[28] Dallas R.W.A., *Architectural and archaeological photogrammetry*, [in:] K.B. Atkinson (ed.), *Close Range Photogrammetry and Machine Vision*, Whittles Publishing, Caithness, U.K. 1996, 283–302.

[29] Hanke K., Grussenmeyer P., *Architectural photogrammetry: Basic theory, procedures, tools*, [in:] Y. Egels, M. Kasser (eds.), *Digital Photogrammetry*, Taylor & Francis, London 2002, 300–339, https://www.isprs.org/commission5/tutorial02/gruss/tut_gruss.pdf.

[30] Rouse J.W. Jr., Haas R.H., Schell J.A., Deering D.W., *Monitoring the vernal advancement and retrogradation (green wave effect) of natural vegetation*, "Progress Report no. 7", Remote Sensing Center, Texas A&M University, College Station, https://ntrs.nasa.gov/search.jsp?R=19740022555 [accessed: 15.06.2019].

[31] Wang J., Rich P.M., Price K.P., Kettle W.D., *Relations between NDVI and tree productivity in the central Great Plains*, "International Journal of Remote Sensing" 2004, Vol. 25, No. 16, 3127–3138, doi: 10.1080/0143116032000160499.

Abstract

The El Fuerte de Samaipata site inscribed on the UNESCO World Heritage List presents a pre-Columbian, multicultural history on the surface of a big sandstone rock. There are several ways of creating precise, high-resolution documentation of this rock, including classic geodetic surveys, modern high-definition surveying (terrestrial laser scanning), and close-range photogrammetry. Close-range photogrammetry is a low cost technique, and the detailed RGB documentation provided by it aids architectural and archaeological research.

This paper presents the results of the application of close-range photogrammetry in different light bands (visual, infrared, and thermal). Sony ILCE-7RM2, Parrot Sequoia, and Flir Tau2 cameras were used. The authors obtained over 50 thousand images and over 27 thousand multispectral images (multiplied by four bands, which gave over 100 thousand single band images). The multispectral and thermal data enabled risk maps to be created for conservation purposes.

Key words: photogrammetry, Samaipata, heritage documentation, rock art

Streszczenie

Wpisane na Listę Światowego Dziedzictwa UNESCO El Fuerte de Samaipata jest świadectwem bogatej, wielokulturowej, prekolumbijskiej historii rzeźbienia tej wielkiej piaskowcowej skały. Opisano zastosowanie wielu sposobów precyzyjnej dokumentacji całej skały, w tym klasyczne metody geodezyjne, nowoczesne pomiary w wysokiej rozdzielczości (naziemne skanowanie laserowe) i fotogrametrię bliskiego zasięgu. Fotogrametria bliskiego zasięgu jest techniką niskokosztową, a dostarczona przez nią szczegółowa dokumentacja RGB pomaga w badaniach architektonicznych i archeologicznych.

W artykule przedstawiono wyniki zastosowania fotogrametrii bliskiego zasięgu w różnych pasmach promieniowania elektromagnetycznego (widzialnym, podczerwonym i termicznym). Zastosowano kamery Sony ILCE-7RM2, Parrot Sequoia i Flir Tau2. Autorzy zebrali ponad 50 tysięcy obrazów RGB i ponad 27 tysięcy obrazów multispektralnych, co pomnożone przez cztery rejestrowane pasma dało w sumie ponad 100 tysięcy pojedynczych obrazów do przetworzenia. Dane multispektralne i termiczne były szczególnie przydatne przy opracowaniu map ryzyka w celach konserwatorskich.

Słowa kluczowe: fotogrametria, Samaipata, dokumentacja zabytków, sztuka naskalna